2020 16th International Conference on
Control, Automation, Robotics and Vision (ICARCV)
December 13-15, 2020. Shenzhen, China

Fractional PI controller for Integrating Plants

Sheikh Izzal Azid
School of Engineering and Physics
The University of the South Pacific
Suva, Fiji
sheikh.azid@usp.ac.fj

Vivek Pawan Shankaran
School of Engineering and Physics
The University of the South Pacific
Suva, Fiji
s11132043@student.usp.ac.fj

Utkal Mehta, *SMIEEE*
School of Engineering and Physics
The University of the South Pacific
Suva, Fiji
utkal.mehta@usp.ac.fj

***Abstract*—This paper verifies a fractional-order PI controller to stabilize integrating time delay plants. Firstly, the stability region by non-integer order controller namely, PI^{λ} is illustrated using boundary condition. This is achieved using complex root boundary domains. The controller parameters are calculated using the ITAE criterion for integrating plant with time delay. The twin rotor MIMO system (TRMS) as an integrating plant is verified in our study. Another example with large time delay is studied to check the validity of fractional-order integrator. Both simulation and experimental results are discussed and compared by PI^{λ} with classical PI. The result proves the effectiveness of the fractional order controller.**

***Index Terms*—Fractional controller, PI^{λ}, Stability, Integrating plant, TRMS.**

I. Introduction

The basic idea of Fractional order calculus (FOC) originated in 1965 [1]. Many researchers have worked on fractional order calculus and have developed different forms of fractional order derivative and integral operators. Recently, the growth and application of FOC has attracted great interest in control engineering and system theory. Nowadays, FOC application for control engineering is considered an emerging area in research [2].

The FOC research focuses mostly on the design problem of the fractional order controller. When the FOC is used, part of the action resembles adding more tuning parameters which gives better outcomes [3]. Authors [4] and [5] discussed the $PI^{\lambda}D^{\mu}$ controller involving real values of λ and μ for integral and derivative orders, respectively. In general, such fractional PID action is widely known now $PI^{\lambda}D^{\mu}$ [6]. It has been proven that a better performance is obtained because of additional control tuning parameters [7]. Studies have shown that the fractional degree is capable to handle even unstable system well, while the classical approach fails to achieve the performance [8]. Moreover, the PD^{μ} is also proposed by [9] to stabilize integrating time delay systems and proved to work better than classical PD. The work has also been done on the fractional order modelling (FOM). Shalaby et al. [10] proposed to use FOM for under-actuated inverted pendulum. The result was compared with integer order model (IOM). Arya and Chakrabarty [11] also discussed fractional order internal model controller with time delay model for desired gain and phase conditions.

Out of many possibilities, PID control strategies are commonly used in process industries due to its simplicity and robust performance in wide range of operating conditions. Among the PID controller, depending on the plant, the whole three terms K_p, K_i and K_d are not necessarily desirable and two terms are chosen (K_p and K_i) commonly. It is important to note that the PD has mostly been applied for integrating plants. This is simply because the integrating term is not satiable to tune for some type of plants and hence, it is eliminated. Nevertheless, the robustness of the system is compromised in this case.

This paper focuses on a fractional PI controller (known as PI^{λ}) to control the integrating plants. Firstly, the PI^{λ} controller is designed for the general integrating plant with time delay. The stabilization for the PI^{λ} is presented by obtaining the stability region of ($K_p,\ K_i$) plane for different values of λ. The presented method is applied to the TRMS plant in the laboratory which is an highly integrating system. The values of K_p, K_i and λ are obtained using ITAE criterion for integrating plant model. The simulation and experimental results are presented in Section IV, and finally the paper is concluded.

II. Stabilization using PI^{λ}

Consider the unity feedback fractional order controlled system as shown in Fig. 1, where $G(s)$ is the integrating time delay system. Let us describe by

$$G(s) = \frac{K}{a_n s^n + a_{n-1}s^{n-1} + \cdots + a_1 s} e^{-\theta s} = \left(\frac{K}{\sum_{i=1}^{n} a_i s^i}\right) e^{-\theta s} \tag{1}$$

where a_i are constants, θ represents the time delay and K represents the static gain. Similarly, let us consider PI^{λ}

978-1-7281-7709-0/20/$31.00 ©2020 IEEE

controller's transfer function as

$$C(s) = K_p + \frac{K_i}{s^\lambda} = \frac{K_p s^\lambda + K_i}{s^\lambda} \tag{2}$$

where K_p is the proportional gain constant, K_i is integrating gain constant and λ is the positive real order of integrator.

The overall transfer function of the system for the unity feedback is given by

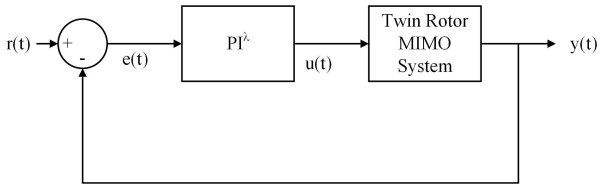

Fig. 1. A simple closed loop control scheme

$$\frac{Y(s)}{R(s)} = \frac{C(s)G(s)}{1 + C(s)G(s)} \tag{3}$$

After substituting (1) and (2) into (3), one can get the following equation.

$$\frac{Y(s)}{R(s)} = \frac{(K_p + \frac{K_i}{s^\lambda})Ke^{-\theta s}}{\sum_{i=1}^{n} a_i s^i + (Ke^{-\theta s})(K_p + \frac{K_i}{s^\lambda})} \tag{4}$$

Thus, the fractional order characteristic equation of the control system can be represented as

$$P(s) = Ke^{-\theta s}\left(\frac{K_p s^\lambda + K_i}{s^\lambda}\right) + \sum_{i=1}^{n} a_i s^i \tag{5}$$

The closed loop system having no right-half plane means the system is stable. The stability domain is defined as the region, when K_p , K_i and λ are members of the domain. The boundaries between stability and instability domains are defined by [9]

1) Real Root Boundary (RRB): The real root boundary is obtained by substituting $s = 0$ in the $P(s)$. This is where the real root crosses the imaginary axis at $s = 0$
2) Complex Root Boundary (CRB) : The complex root boundary is obtained by substituting $s = j\omega$ in the $P(s)$. The real and imaginary part of the $P(s)$ is equated to zero simultaneously.
3) Infinite Root Boundary (IRB): The infinite root boundary is obtained by substituting $s = j\infty$ in the $P(s)$.

The PI^λ is obtained by constructing the CRB when jw is substituted for s. For this closed loop system, RRB and IRB are not applicable. One can obtain the following expression,

$$P(jw) = Ke^{-\theta jw}(\frac{K_p jw^\lambda + K_i}{jw^\lambda}) + \sum_{i=1}^{n} a_i jw^i \tag{6}$$

After removing the non-integer power of a complex number $(jw)^\lambda$, it gives

$$P(jw) = K(cos\omega\theta + jsin\omega\theta)[K_p + \frac{K_i}{\epsilon + j\zeta}] + \sum_{i=1}^{n} a_i(\varsigma_i + j\kappa_i) \tag{7}$$

where

$$\epsilon = \Re P(jw)^\lambda; \zeta = \Im P(jw)^\lambda$$
$$\varsigma = \Re P(jw)^i; \kappa = \Im P(jw)^i; i = 1...n$$

Equating the real and imaginary parts of (7) to zero

$$\begin{aligned} K_p E(\omega) + K_d C(\omega) &= -\textstyle\sum_{i=1}^{n} a_i(\varsigma_i) \\ K_p F(\omega) + K_d D(\omega) &= -\textstyle\sum_{i=1}^{n} a_i(\kappa_i) \end{aligned} \tag{8}$$

where

$$\begin{aligned} E &= Kcos(\omega\theta) \\ F &= -Ksin(\omega\theta) \\ C &= K\epsilon cos(\omega\theta) + K\zeta sin(\omega\theta) \\ D &= K\zeta cos(\omega\theta) - K\epsilon sin(\omega\theta) \end{aligned}$$

Thus, by solving the 2-dimensional system of (8), the expression of K_p and K_i for the PI^λ is

$$\begin{aligned} K_p &= \tfrac{\epsilon^2 - \zeta^2}{K^2\zeta}[\textstyle\sum_{i=1}^{n} a_i\varsigma_i D(\omega) - \sum_{i=1}^{n} a_i\kappa_i C(\omega)] \\ K_i &= \tfrac{\epsilon^2 - \zeta^2}{K^2\zeta}[\textstyle\sum_{i=1}^{n} a_i\kappa_i E(\omega) - \sum_{i=1}^{n} a_i\varsigma_i F(\omega)] \end{aligned} \tag{9}$$

These equations could then be used to construct the CRB of any particular integrating system in-order to effectively identify its stability region. By changing ω from 0 to ∞, a stability boundary root locus is constructed in the K_p, K_i plane.

III. Verification

In this section, the results with simulation example will be given to illustrate the effect of the parameter λ. It will show the stability of integrating plant with PI^λ.

A. Example 1 : Twin Rotor MIMO System

Let us take the model of the Yaw transfer function of TRMS. It is a $3rd$ order integrating plant and is unstable with a PI controller.

The TRMS model shown in Fig. 2 has two rotors; the horizontal rotor is for yaw movement and the vertical rotor is for pitch movement. Both the rotors are connected to the ends of the beam which is free to move in horizontal and vertical planes. The equilibrium point of the beam is decided by a counterbalance and one end of its arm is connected to the beam at the pivot and the other end with a weight. Both the rotors are driven by DC motors. The yaw and pitch movement can be restricted to 1 DOF by detaching one of the rotors.

The complete dynamics of the TRMS system can be represented as follows [12].

Fig. 2. The Twin Rotor MIMO System

TABLE I
TRMS PARAMETERS

Parameter	Symbol	Value
Moment of Inertia Vertical Rotor	I_1	$6.8.10^2 kg.m^2$
Moment of Inertia Horizontal Rotor	I_2	$2.10^2 kg.m^2$
Static characteristic parameter	a_1	0.0135
Static characteristic parameter	b_1	0.0924
Static characteristic parameter	a_2	0.02
Static characteristic parameter	b_2	0.09
Gravity momentum	M_g	$0.32Nm$
Friction momentum function	B_{1a_v}	$6.10^{-3} Nms/rad$
Friction momentum function	B_{2a_v}	$1.10^{-3} Nms/rad$
Friction momentum function	B_{1a_h}	$1.10^{-1} Nms/rad$
Friction momentum function	B_{2a_h}	$1.10^{-2} Nms/rad$
Gyroscopic	K_{gy}	$0.05s/rad$
Vertical motor gain	k_1	1.1
Horizontal motor gain	k_2	0.8
Vertical motor denominator parameter	T_{11}	1.1
Vertical motor denominator parameter	T_{10}	1
Horizontal motor denominator parameter	T_{21}	1
Horizontal motor denominator parameter	T_{20}	1
Cross reaction parameter	T_p	2
Cross reaction parameter	T_0	3.5
Cross reaction momentum gain	k_c	-0.2

Mathematical equation for the vertical plane

$$\begin{aligned} I_1\dddot{\psi} &= M_1 - M_{FG} - M_G \\ M_1 &= a_1\tau_1^2 + b_1\tau_1 \\ M_{FG} &= M_g sin\psi \\ M_{B\psi} &= B_{1\dot{\psi}} + B_2 sin(\dot{\psi}) \\ M_G &= K_{gy} M_1 \dot{\psi} cos(\psi) \end{aligned} \tag{10}$$

where M_1 is non-linear static characteristics, M_G is the gyroscopic momentum and M_{FG} is the gravity momentum. The vertical rotor momentum is described as $\tau_1 = \frac{k_1}{T_{11}s+T_{10}}u_1$

The same method is applied for the horizontal plane

$$\begin{aligned} I_2\dddot{\psi} &= M_2 - M_{B\phi} - M_R \\ M_2 &= a_2\tau_2^2 + b_2\tau_2 \\ M_{B\phi} &= B_{1\dot{\phi}} + B_2 sin(\dot{\phi}) \\ M_R &= \frac{k_c(T_0 s+1)}{T_P s+1}\tau_1 \end{aligned} \tag{11}$$

where M_R is the reaction momentum and the vertical rotor momentum is given as $\tau_2 = \frac{k_2}{T_{21}s+T_{20}}u_2$

For the purpose of this paper, we will focus only on the control of the yaw movement, which is 1 DOF. Thus, the transfer function of the horizontal plane is shown in (12).

$$G(s) = \frac{K}{a_3 s^3 + a_2 s^2 + a_1 s} e^{-\theta s} \tag{12}$$

where $K = 3.6$, $a_3 = 1$, $a_2 = 10$, $a_1 = 6$ and $\theta = 0.05$. The stability region for various region of λ in the PI^λ controller will be implemented.

The fractional order for characteristic equation of the control system is derived by

$$P(s) = 3.6e^{-0.05s}(K_p + \frac{K_i}{s^\lambda}) - 6s + 10s^2 + s^3 \tag{13}$$

After solving for K_p and K_i, as per (9), the stability region for the PI^λ was plotted for different λ values.

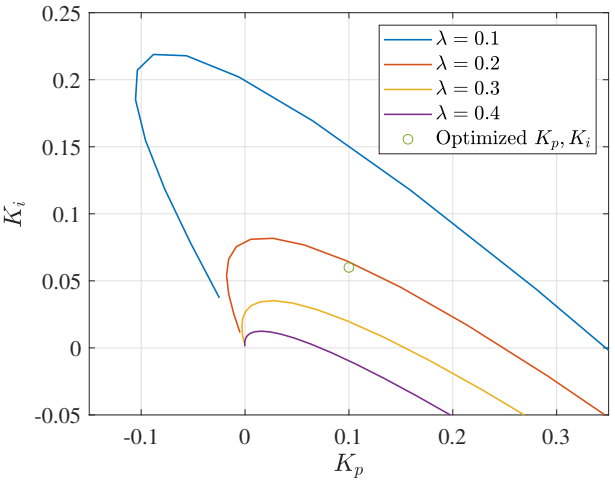

Fig. 3. Stability Region for PI^λ controller

Fig. 3 shows the stability boundary ranges for the different λ values. The λ is plotted from the range between $0.1 \leq \lambda < 1$. To note that when λ = 1, it behaves as classical PI controller. For the case of twin rotor, it is found that the λ between 0.1 to 0.4 has the stability region and beyond 0.4, the PI^λ does not provide the stability and suitable gain values. Therefore, it is suitable to select the range between 0.1 to 0.4. For the values 0.5 to 0.9, the stability boundary is in the negative region, which is undesirable.

To show the effect of the PI^{λ} controller, the λ out of the values between 0.1 to 0.4, the value of 0.1 is chosen for this case, as it has wider range of the stability boundary. Thus, the fractional controller for the Twin Rotor system is $PI^{0.1}$. Also, any K_p and K_i in this stability region for the plant would be reliable. Now, the ITAE is commonly referred to as a good performance index in designing PID controllers [13]. The ITAE function is given by

$$J = \int_0^{\infty} t|e(t)|dt \tag{14}$$

Out of many possibilities, ITAE index is applied to choose the optimal K_p and K_i gains in this study.

B. Example 2

Consider a second order integrating system with delay such as

$$G(s) = \frac{K}{s(s+a)}e^{-\theta s} = \frac{K}{a_2 s^2 + a_1 s}e^{-\theta s} \tag{15}$$

where $K = 2$, $a_2 = 1$, $a_1 = 5$ and $\theta = 1$.

Hence, the fractional order for the characteristic equation of the control system is derived by

$$P(s) = 2e^{-1}(\frac{K_p s^{\lambda} + K_i}{s^{\lambda}}) + 5s + s^2 \tag{16}$$

The stability boundary for the above (16) is

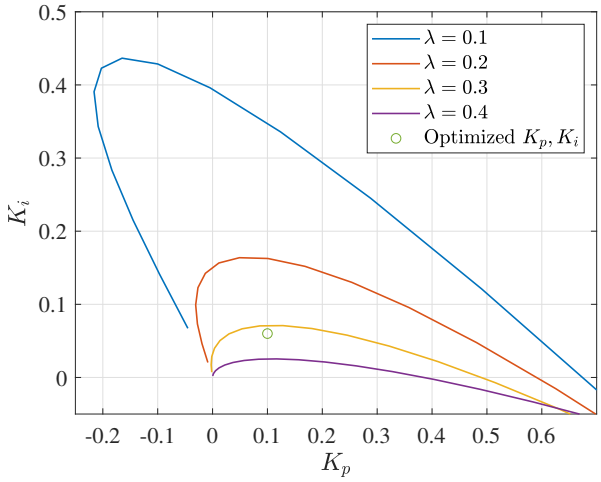

Fig. 4. Stability Region for PI^{λ} controller

The CRB curve is plotted for $0.1 \leq \lambda < 1$. Moreover, Fig. 4, shows the λ from 0.1 to 0.4 would make the system stable. Thus, by using the λ range with ITAE, the $K_p = 0.346$, $K_i = 0.15$ and $\lambda = 0.147$

IV. Result and Discussion

A. Example 1 : Twin Rotor MIMO System

From the CRB plot of Fig. 3, the stability boundaries were obtained for $\lambda = 0.1$ which were used to determine the parameter ranges of K_p and K_i. The ranges of the FOPI gains were selected to be $K_p \in (0, 0.35)$ and $K_i \in (0, 0.2)$. The parameters were then optimized using ITAE method by MATLAB's FOMCON toolbox using FPID Optimization toolbox. The optimized gains were obtained as $K_p = 0.1$ and $K_i = 0.06$.

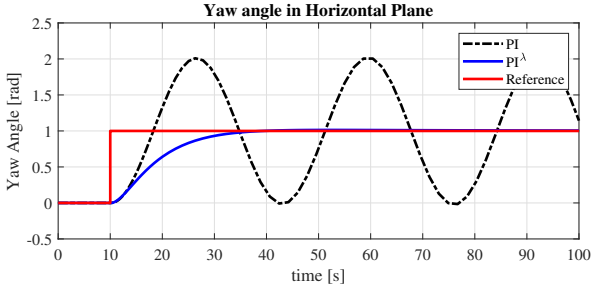

Fig. 5. Comparison of PI^{λ} with classical PI in Simulation

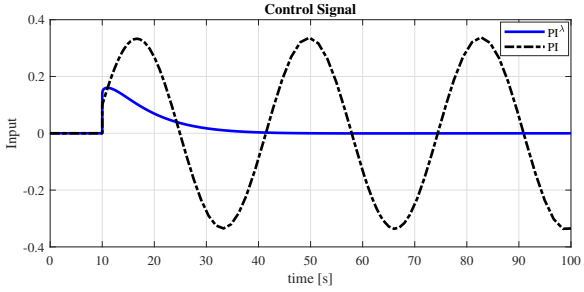

Fig. 6. Control Signal of the PI^{λ} vs classical PI in Simulation

The simulation results, using only the horizontal rotor of the Twin Rotor MIMO system, is shown in Fig. 5. The control input variations are plotted in Fig. 6. The PI^{λ} controller shows satisfactory result, however, the classical PI controller is unstable. This is because the PI controller acts on the integrating system, which is not applicable. The reference is $1rad/s$ and the PI^{λ} achieves steady state response. It can be noted that PI^{λ} works perfectly with the integrating plant while, maintaining the robustness of the control. Also, the behaviour of the PI^{λ} is computed with adding a disturbance of $0.5rad$.

Fig. 7 shows the result of the PI^{λ} with the added disturbance at $60s$. The fractional controller is able to compensate the disturbance and achieve the desired yaw angle. The comparison of experimental results between PI^{λ} and classical PI is also presented in the figure. It is clearly revealed that PI^{λ} has kept the stability in closed loop performance and

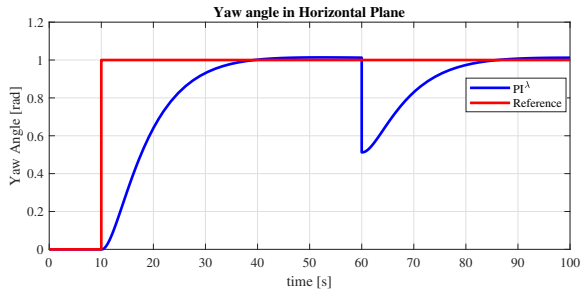

Fig. 7. Performance of PI^{λ} with -0.5 rad disturbance

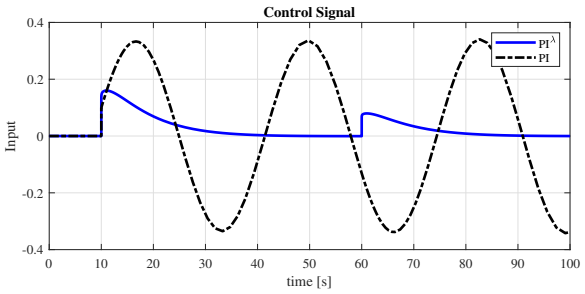

Fig. 8. Control Signal of the PI^{λ} in Simulation with Disturbance

achieved steady state in approximately 27sec. However, it was difficult to conduct the experiment using classical PI on the same TRMS plant. The result was highly unstable. The experimentation of classical PI was stopped at $60s$ to avoid damage to the experiment setup. On the contrary, the PI^{λ} controller perfectly stabilized with real-time hardware setup. The control signal variation with PI^{λ} in Fig. 8 is acceptable. From this result, it can be concluded that PI^{λ} controller would work for integrating plants.

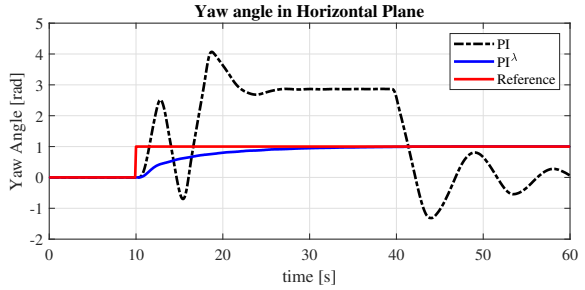

Fig. 9. Comparison of PI^{λ} with classical PI in Experimentation

B. Example 2

To add on, from Fig. 4, the stability boundary gives the range of the λ. With this information, by using FOMCOM toolbok and ITAE optimization, the $K_p = 0.346$, $K_i = 0.15$ and $\lambda = 0.147$. The simulation result is presented in Fig. 11 and Fig. 12.

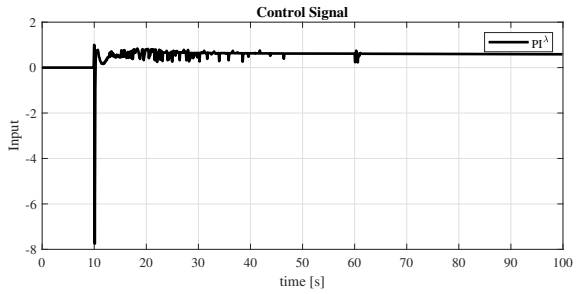

Fig. 10. Control Signal of the PI^{λ} in Experimentation

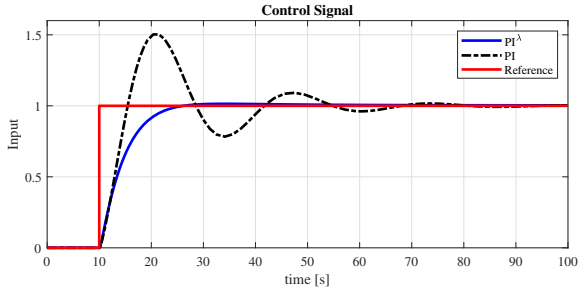

Fig. 11. Comparison of PI^{λ} with classical PI in Simulation

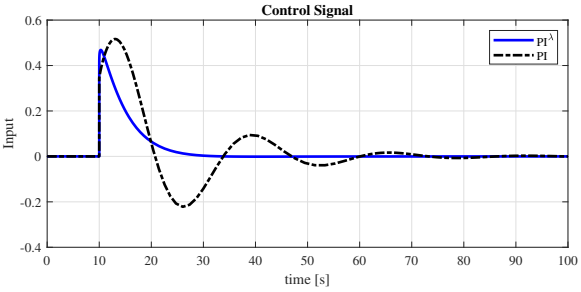

Fig. 12. Control Signal of the PI^{λ} vs classical PI in Simulation

The simulation results prove that PI^{λ} performs better than classical PI even with a different type of integrating system with greater delays. With the step input of 1 given to the proposed example, the classical PI stabilizes after 70s while the PI^{λ} is able to achieve this in 20s. Also, note that the classical PI is optimised to give the best response. This actually proves that the proposed method works with all types of integrating plants.

V. Conclusion

In this paper, the PI^{λ} controller is proposed to control integrating plants when the classical PI failed to achieve the result. This method discusses the stability of the generalized integrating systems. The CRB graph is plotted for different λ values to check the stability with PI^{λ}.

REFERENCES

[1] G. Teodoroa, J. Machado, and E. C. de Oliveira, "A review of definitions of fractional derivatives and other operators," *Journal of Computational Physics*, vol. 388, pp. 195–208, 2019.

[2] K. Kothari, U. Mehta, and R. Prasad, "Fractional-order system modeling and its applications," *Journal of Engineering Science and Technology Review*, vol. 12(6), pp. 1–10, 2019.

[3] A. Singh, D. Deb, and H. Agrawal, "On selection of improved fractional model and control of different systems with experimental validation," *Communications in Nonlinear Science and Numerical Simulation*, vol. 79, 06 2019.

[4] I. Podlubny, "Fractional-order systems and PI$^{\lambda}D^{\mu}$ controllers," *IEEE Transactions on Automatic Control*, vol. 44, no. 1, pp. 208–214, 1999.

[5] G. Gurumurthy and D. Das, "An FO-I$^{\lambda}D^{1-\lambda}$ controller design and realization for inverted decoupled two input two output-liquid level system," *International Journal of Dynamics and Control*, vol. 8, pp. 1013–1026, 01 2020.

[6] M. Charef and A. Charef, "Fractional order controller based on the fractionalization of PID controller," in *2017 5th International Conference on Electrical Engineering - Boumerdes (ICEE-B)*, 2017, pp. 1–5.

[7] U. Mehta, V. Lechappe, and O. P. Singh, *Simple FOPI tuning Method for real-order time delay systems*. Springer Singapore, 2018, vol. 442, pp. 459–468.

[8] K. Kothari, U. Mehta, and N. Singh, "Practical test for closed-loop identification and control on magnetic levitation system: A fractional-order approach," in *2018 15th International Conference on Control, Automation, Robotics and Vision (ICARCV)*, 2018, pp. 1805–1810.

[9] S. Hamamci, "Calculation of all stabilizing fractional order PD controllers for integrating time delay systems," *Computers and Mathematics with Applications*, vol. 59, pp. 1621–1629, 03 2010.

[10] R. Shalaby, M. El-Hossainy, and B. Abo-Zalam, "Fractional order modeling and control for under-actuated inverted pendulum," *Communications in Nonlinear Science and Numerical Simulation*, vol. 74, pp. 97–121, 03 2019.

[11] P. P. Arya and S. Chakrabarty, "A robust internal model-based fractional order controller for fractional order plus time delay processes," *IEEE Control Systems Letters*, vol. 4, no. 4, pp. 862–867, 2020.

[12] S. Chaudhary and A. Kumar, "Control of twin rotor mimo system using 1-degree-of-freedom PID, 2-degree-of-freedom PID and fractional order PID controller," in *2019 3rd International conference on Electronics, Communication and Aerospace Technology (ICECA)*, 2019, pp. 746–751.

[13] F. Zhang, C. Yang, X. Zhou, and W. Gui, "Optimal setting and control strategy for industrial process based on discrete-time fractional-order PI$^{\lambda}$ D$^{\mu}$," *IEEE Access*, vol. 7, pp. 47 747–47 761, 2019.